

RESEARCH ARTICLE

Possible relationship between heatwaves in Korea and the summer blocking frequency in the Sea of Okhotsk

Jae-Won Choi¹ | Chan-Yeong Song²  | Eung-Sup Kim² | Joong-Bae Ahn² 

¹Institute for Basic Science, Pusan National University, Busan, South Korea

²Division of Earth Environmental System, Pusan National University, Busan, South Korea

Correspondence

Joong-Bae Ahn, Division of Earth Environmental System, Pusan National University, Geumjeong-gu, Busan, 46241, Republic of South Korea.
Email: jbahn@pusan.ac.kr

Funding information

Rural Development Administration, Grant/Award Number: PJ01489102

Abstract

This study examined the relationship between heatwaves in Korea and blocking in the Sea of Okhotsk (OK) region, which significantly influences the Korean climate in summer. According to the analysis, negative correlations were observed between the blocking frequency in the OK region and heatwave days (HWD) and the surface air temperature (SAT) in Korea over the past four decades (1979–2018). These negative correlations suggest that when the blocking frequency in the OK region increases in summer, the HWD and SAT decrease in Korea. This study selected 10 years of high blocking frequency years (high BF years) and 10 years of low blocking frequency years (low BF years) and analysed the differences between the two groups to explain the negative relationship between the HWD in Korea and the blocking frequency in the OK region. The difference between the two groups revealed strong anomalous anticyclonic and cyclonic circulations that developed in the north Siberia region and northeast Australia (NEA), respectively, throughout all layers in the troposphere. The large anomalous anticyclonic pattern in the North Siberia region was related to the blocking high, while the anomalous cyclonic pattern that developed in NEA was related to the East Asian summer monsoon (EASM) front. The difference in the sea surface temperature (SST) between the two groups was also analysed. In the North Atlantic Ocean, a tripole structure appeared with a cold anomaly in the high latitudes, a warm anomaly in the mid-latitudes and a cold anomaly again in the low latitudes, which is a typical spatial distribution of the SST anomaly related to the positive North Atlantic Oscillation (NAO) phase.

KEYWORDS

blocking, east Asian summer monsoon, heatwave days, North Atlantic oscillation, sea of Okhotsk

1 | INTRODUCTION

The unusually high summer temperature has a substantial negative impact on human health and hygiene, as well as on all aspects of daily life and social activities. Heatwaves refer to extremely high temperatures lasting

for several days, which can cause heat stress and, even worse, heat stroke to humans and ecosystems. In addition, heatwaves at night aggravate heat stress, reducing work efficiency and quality of life by interfering with comfortable sleep. Recently, abnormal and record-high heatwaves have increased in the Korean Peninsula, and

various damage has been reported. In particular, abnormally high temperatures in 1994 and 2018 focused attention on heatwaves (Yeh *et al.*, 2018; Ha *et al.*, 2020). In 2018, a strong and long-lasting heatwave with record-breaking surface daily maximum temperature was observed in Korea. The daily maximum temperature in Seoul, the capital of the Republic of Korea, reached a historical record of 39.6°C. In Hongcheon, a rural area in Gangwon Province, the daily maximum temperature rose to 41.0°C, setting a national record. In addition, a national average daily maximum temperature of over 33°C was recorded for 31.5 days and tropical nights with a daily minimum temperature of over 25°C, which lasted for 17.7 days. The recent scenario study (IPCC Six assessment report) using climate models has suggested that the heatwave frequency will increase globally in the 21st century according to global warming (National Institute of Meteorological Studies (NIMS), 2016).

Kim *et al.* (1998) reported that heatwaves occur when the Korean Peninsula is located in the center of the high pressure followed by the abnormal movement of western North Pacific subtropical high (WNPSH) to the north, resulting in adiabatic compression along with the downward flows, causing high temperatures in the region. Byun *et al.* (2006) attributed the abnormal heat in the southeastern inland region of South Korea (Miryang area) in 2004 to the stronger-than-normal development of WNPSH, resulting from the second circulation induced by typhoons and the reduced snow cover over the Tibetan Plateau. They insisted that these produced a high pressure in the southwest sea of Korea, resulting in the movement of the axis of the high-temperature area to the south. They examined the causes of the high-temperature event in terms of the meso-to-large-scale atmospheric circulation.

Several studies have examined the high temperatures caused by local effects in South Korea. Lee (1994) reported that the high temperatures in the western part of the Taebaek Mountains, which crosses the Korean Peninsula from north to south, are caused by topographical effects called the föhn phenomenon when easterlies are crossing the mountain range. Kim and Hong (1996) showed that high temperatures appeared in the eastern part of the range when the westerlies crossed the mountains for the same reason. Kim and Min (2001) reported that adiabatic heating caused by the downward sinking flows, which formed to compensate for the upward rising flows climbing on the slopes of mountains when the westerly wind blew, is a major local mechanism for the high temperatures in the Daegu region, an inland basin in the southeastern part of the Korean Peninsula. They insisted that the temperature rise enhanced by the terrain effect was up to 10 times or higher than that without the terrain. Lee (2003) reported that the temperature on the

west coast was higher than that on the east coast when the easterly wind blew in summer. The föhn phenomenon was likely to occur in the western slope of the Taebaek Mountains that cross the Korean Peninsula from north to south along the east coast because of relatively high-saturated vapour pressure and cloud cover in the east coast. These studies show that topographical influences can contribute to localized high temperatures in South Korea.

Studies on the causes of heatwaves in Korea have increased in recent years owing to the recent increase in the intensity of heatwaves and accelerating global warming. Lee and Lee (2016) analysed the interannual variation of heatwaves in Korea and the related large-scale atmospheric circulation patterns. Kim *et al.* (2019) investigated the effect of diabatic heating over the Indian subcontinent and the Tibetan Plateau sensible heat on heatwaves in Korea. Yeo *et al.* (2019) showed that most heatwaves in Korea could be classified into two types based on the spatial pattern of atmospheric circulation anomalies: zonal and meridional wave types. Yoon *et al.* (2020) divided the synoptic pattern caused by the heatwave events during the recent 38 years (1981–2018) into three clusters utilizing a clustering method. They analysed the trend of the heatwaves in each cluster. Yeh *et al.* (2018) examined the causes of the record-breaking heatwave in 2016 in Korea. They suggested that the heatwave was caused by blocking that developed in the Kamchatka Peninsula. Lim and Seo (2019) developed a statistical model to predict an extreme summer temperature in Korea using the sea surface temperature (SST) in North Atlantic, western North Pacific and eastern North Pacific. Hong *et al.* (2018) examined the features of the large-scale atmospheric circulation, which caused the heatwaves and tropical nights in Korea. Tropical nights are defined as the number of days with the lowest night temperature above 25°C. Ha *et al.* (2020) made an effort to define the cause of the unprecedentedly hot summer in 2018. They singled out the continuation of the anticyclone, which was strong and extended to the northwest of Korea by August 2018, as the cause of the extraordinarily hot 2018.

On the other hand, except for a few case studies, few studies on climatological analysis on the relationship between heatwaves in Korea and summer blocking have been reported. Therefore, this study examined the climatic effect of blocking in the Okhotsk Sea region, which is believed to be a major cause of summer heatwaves on the Korean Peninsula.

In Section 2, the data and analysis methods are introduced. Section 3 explains the relationship between summer blocking frequency and heatwaves in Korea. The blocking mechanism in the Sea of Okhotsk region, which is the cause of the heatwaves in Korea, is presented in Section 4. Finally, Section 5 reports the conclusions of this study.

2 | DATA AND METHODOLOGY

2.1 | Data

This study utilized the surface air temperature (SAT) and precipitation observed at 58 in situ weather stations in South Korea and the Palmer Drought Severity Index

(PDSI) data obtained from those observations. These data were obtained from the website (<https://www.kma.go.kr>) of the Korea Meteorological Administration (KMA). Figure 1a presents the spatial distribution of 58 weather observation stations. The data observed on islands far from the Korean Peninsula were excluded from the analysis, assuming that their characteristics were different

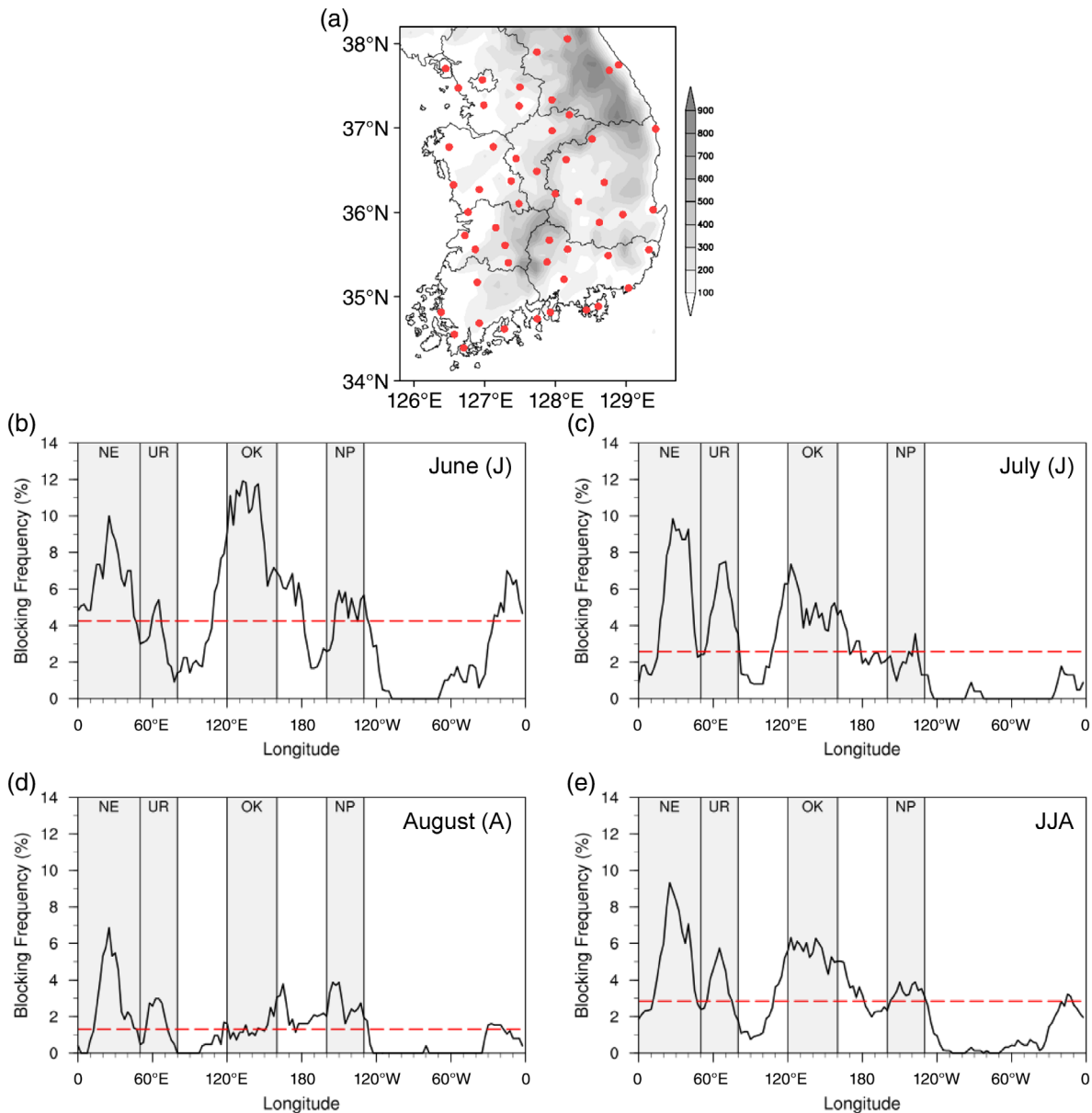


FIGURE 1 (a) Topography (unit: m) and spatial distribution of weather observation stations in Korea. Climatology of the blocking frequency in (b) June, (c) July, (d) August and (e) June–August (JJA) for the period of 1979–2018. The red dashed line indicates the average for all longitudes. ‘NE’, ‘UR’, ‘OK’ and ‘NP’ denote North Europe, Ural region, Okhotsk Sea and northeastern Pacific, respectively [Colour figure can be viewed at wileyonlinelibrary.com]

from those of inland areas. The number of HWDs and tropical night days (TNDs) in Korea were provided officially on the website of the KMA (<https://data.kma.go.kr/climate/>). The KMA defines the HWD as the number of days with daily highest temperatures above 33°C and the TND as the number of days with lowest night temperatures above 25°C.

For the analysis of large-scale environments and atmospheric circulation, the Reanalysis-2 (R-2) daily and monthly average data from 1979 to 2018 distributed by the National Centers for Environmental Prediction (NCEP)-Department of Energy (DOE) were used (Kanamitsu *et al.*, 2002). The data have a latitude–longitude $2.5^\circ \times 2.5^\circ$ grid horizontal resolution and 17 vertical layers. The monthly global SST data were from National Oceanic and Atmospheric Administration (NOAA) Extended Reconstructed SST analysis (version 3; Smith *et al.*, 2008). The NOAA interpolated outgoing longwave radiation (OLR) was used for the convective activity analysis (Liebmann and Smith, 1996). The precipitation data used were obtained from Global Precipitation Climatology Project (GPCP) version 2.3 (Adler *et al.*, 2003). The East Asian summer monsoon (EASM) index (EASMI) used in this study was the one used by Li and Zeng (2002, 2003, 2005). The EASMI was defined using the Dynamical Normalized Seasonality (DNS) index of Li and Zeng (2002, 2003, 2005). The basic concept of the DNS index is based on the intensity of the normalized seasonality of wind fields. Since monsoons have very strong seasonal variations of wind directions defining strong and weak monsoons using the magnitude of the seasonality of wind fields is reasonable. Using this basic concept of monsoons, the DNS index is calculated through the following equation.

$$\delta_{mn} = \frac{\|\bar{V}_1 - V_{mn}\|}{\|\bar{V}\|} - 2$$

where, \bar{V}_1 and \bar{V} refer to the January climatological wind vector and the January and July climatological wind vectors respectively and V_{mn} refers to the monthly wind vector for year n and month m . Hereinafter, the EASMI is defined as the area-averaged seasonally (June–August) DNS at 850 hPa in the East Asian monsoon domain (10° – 40° N, 110° – 140° E).

2.2 | Methodology

In this study, tropical storm (TS) developed in the western North Pacific whose maximum sustained wind

speed (MSWS) was more than 17 m/s is defined as TC. In addition, in this study, the cyclone, which was once a TC in the low latitudes and then downgraded to an extratropical cyclone (EC) as it moved northward, was also considered a TC because it could still cause significant damage.

A two-tailed Student's t -test was used to determine the significance of the results in this study (Wilks, 1995). In this study, summer means June, July and August. The duration of Changma, called Meiyu in China and Baiu in Japan, was defined as the period from when precipitation related to the rainy season began in the southern part of the Korean Peninsula to when it ended in the central part of the peninsula.

2.3 | Definition of the blocking index

The blocking in this study was defined using the index employed in the meridional geopotential height gradients proposed by Barriopedro *et al.* (2006). This index is based on the method proposed in Tibaldi and Molteni (1990) and used in many previous studies (e.g. You and Ahn, 2012; Park and Ahn, 2014; Choi and Ahn, 2017; Lee and Ahn, 2017). The daily blocking index was calculated using the daily averaged 500 hPa geopotential height obtained from R-2. For each longitude, the northern 500 hPa geopotential height gradient (GHGN) and the southern 500 hPa geopotential height gradient (GHGS) are defined as follows:

$$GHGN(\lambda) = \frac{Z(\lambda, \phi_N) - Z(\lambda, \phi_0)}{\phi_N - \phi_0} \quad GHGS(\lambda) = \frac{Z(\lambda, \phi_0) - Z(\lambda, \phi_S)}{\phi_0 - \phi_S}$$

$$\begin{aligned} \phi_N &= 77.5^\circ\text{N} + \Delta, \phi_0 = 60.0^\circ\text{N} + \Delta, \phi_S = 40.0^\circ\text{N} + \Delta, \\ \Delta &= -5.0^\circ, -2.5^\circ, 0.0^\circ, 2.5^\circ, \text{ or } \\ &5.0^\circ \end{aligned}$$

where $Z(\lambda, \phi)$ refers to the 500 hPa geopotential height at longitude (λ) and latitude (ϕ). A given longitude is considered blocked if $GHGN(\lambda)$ and $GHGS(\lambda)$ simultaneously satisfy the following conditions over at least one of the five different reference latitudes:

$$GHGN < -10 \text{ m } (^\circ\text{latitude}^{-1}),$$

$$GHGS > 0 \text{ m } (^\circ\text{latitude}^{-1})$$

Finally, the blocking event occurred when the above conditions were maintained for at least 5 days in a given

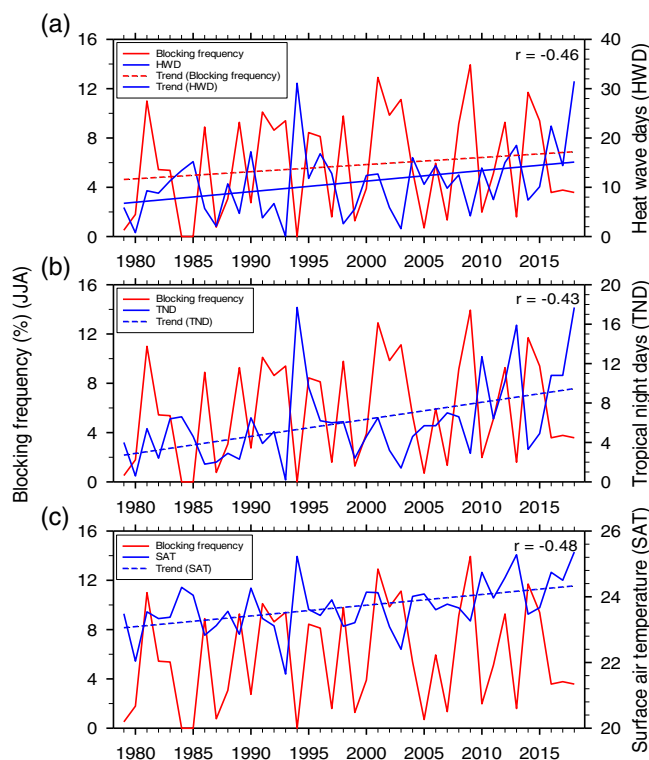


FIGURE 2 Time series of (a) JJA blocking frequency (BF) and heatwave days (HWD), (b) JJA BF and tropical night days (TND) and (c) JJA BF and JJA surface air temperature (SAT) averaged over weather observation stations in Korea [Colour figure can be viewed at wileyonlinelibrary.com]

longitude. The blocking frequency (BF) means the ratio of blocking days to the total number of days.

Figure 1b–e shows the climatological summertime BFs in the longitude in the northern hemisphere. Regions with high BF were Northern Europe (NE, 0° – 50° E), Ural region (UR, 50° – 80° E), Sea of Okhotsk (OK, 120° – 160° E) and Northeastern Pacific (NP, 160° – 130° W). The above result is similar to that reported by Park and Ahn (2014). The climatological BFs in the above regions tended to decrease in summer, particularly in the order of June, July and August. This study examined the relationship between blocking and heatwaves in Korea during June to August in the OK region, which has the most influence on the Korean climate in summer.

3 | RELATIONSHIP BETWEEN BLOCKING FREQUENCY AND HEATWAVE DAYS

Figure 2a shows the time series of the blocking frequency in the OK region in summer and HWDs in Korea from June to August. The blocking frequency showed an increasing tendency up until now. This increasing tendency was statistically significant at the 90% confidence

level. The trend of the blocking frequency was 0.06 yr^{-1} . The HWD also showed a strong increasing tendency, which was significant at the 95% confidence level. The trend of the HWD was $0.2 \text{ day}\cdot\text{yr}^{-1}$. The out-of-phase relationship between these two variables was obvious. According to the correlation between the two variables, a negative correlation of -0.46 was formed, which was significant at the 99% confidence level. This negative correlation suggests that the number of HWDs in summer in Korea decreased when the blocking frequency increased.

The time series of the blocking frequency in the OK region during summer and the number of TND in Korea in summer were also analysed (Figure 2b). The number of TND showed an increasing tendency until now, and this increasing tendency was significant at the 99% confidence level. The trend of TND is $0.2 \text{ day}\cdot\text{yr}^{-1}$. The out-of-phase tendency was also obvious between the two variables. Thus, the correlation between the two variables was analysed. As a result, a negative correlation of -0.43 was observed, which was significant at a 99% confidence level. This negative correlation means that if the blocking frequency increased in the OK region during summer, the summer TNDs decreased in Korea.

This study analysed the time-series of observed SAT averaged over 58 weather observation stations in Korea

during June to August with a blocking frequency in the OK region during the same months (Figure 2c). The summer SAT in Korea showed a steady increase, and the increasing tendency was significant at the 99% confidence level. The trend of SAT was $0.2^{\circ}\text{Cyr}^{-1}$. In addition, the out-of-phase tendency was clear between the two variables. Thus, the correlation between the two variables was analysed. As a result, a negative correlation of -0.48 was revealed, which was significant at the 99% confidence level. The summer SAT decreased in Korea when the blocking frequency increased in the OK region during summer.

This study selected the 10-year high blocking frequency years (high BF years) and 10-year low blocking frequency years (low BF years) and analysed the difference between the two groups to explain the reduction in the number of HWDs in Korea when the blocking frequency in summer in the OK region increased. The selected 20 years accounted for half of the total analysis period, which was 40 years. As listed in Table 1, the average number of HWDs was 5.8 and 12.5 days in the high and low BF years, respectively; the number of HWDs in the low BF years was more than twice that in the high BF years. The difference in the average number of HWDs between the two groups was significant at the 95% confidence level. The number of average TNDs in the high BF and low BF years was 3.8 days and 7.2 days, respectively; the number of TNDs in the low BF years was also more than double that in the high BF years. The difference in the average TNDs between the two groups was significant at the 95% confidence level. The results in Table 1 suggest that the summer HWDs decreased (or increased) as the blocking frequency increased (or decreased) in the OK region in summer, as exhibited in the above correlation analysis results.

TABLE 1 Statistics of heatwave days (HWD) and tropical night days (TND) on high and low BF years

High BF years			Low BF years		
Year	HWD	TND	Year	HWD	TND
1981	9.3	5.4	1979	5.9	4.0
1991	3.8	3.9	1984	13.4	6.6
1993	0.1	0.2	1985	15.2	4.6
1998	2.6	6.1	1987	2.1	2.0
2001	12.7	6.5	1994	31.1	17.7
2002	5.9	3.2	1997	12.8	6.0
2003	1.6	1.4	1999	5.6	2.4
2009	4.2	2.9	2005	10.6	5.7
2014	7.4	3.3	2007	9.8	7.0
2015	10.1	4.9	2013	18.5	15.9
Average	5.8	3.8	Average	12.5	7.2

4 | DIFFERENCES BETWEEN HIGH BF YEARS AND LOW BF YEARS

4.1 | Spatiotemporal variation of precipitation and SAT

The left panel of Figure 3 shows the average spatial distribution of precipitation in the high BF frequency (Figure 3a), the average spatial distribution in the low BF years (Figure 3b), and the spatial distribution of the difference in the average precipitation between high and low BF years (Figure 3c). In the high BF years, more than 300 mm of precipitation occurred in the southern and northern regions except for the central part of South Korea (left panel of Figure 3a). In the low BF years, however, less than 300 mm of precipitation occurred in most regions in South Korea (left panel of Figure 3b). In particular, very little precipitation (148 mm) occurred in the east coast region. The difference in precipitation between the high and low BF years showed a positive anomaly in most regions except for the central region on the west coast (left panel of Figure 3c). The difference in the daily precipitation between the two groups shows that more precipitation occurred in the high BF years from July to mid-August (left panel of Figure 3d). This difference is significant at the 95% confidence level.

In the spatial distribution of SAT in the high BF years, most regions in South Korea exhibited a temperature below 25°C . The lowest SAT was revealed in the northern region of the east coast (right panel of Figure 3a). In the low BF years, the SAT was 25°C or higher in most regions except the northeast region. The highest SAT was observed in the southwest region (right panel of Figure 3b). The spatial distribution of the difference in the SAT between the high and low BF years revealed a cold anomaly in all regions in South Korea (right panel of Figure 3c). The lowest cold anomaly was revealed along the east coastline. In the time series of the difference in the daily SAT between the two groups, a lower SAT was noted in the high BF years from June to mid-November than in the low BF years. The most significant difference was revealed in July to August (right panel of Figure 3d). This difference is significant at the 95% confidence level. This means that SATs decreased more in the high BF years than in the low BF years because of higher precipitation in the high BF years, which was related to the decrease in HWDs.

4.2 | Large-scale environments

Figure 4a shows the difference in 2 m air temperature (Air2m) between the two groups in the Asian regions in summer. Overall, Northeast Asia (NEA) and some

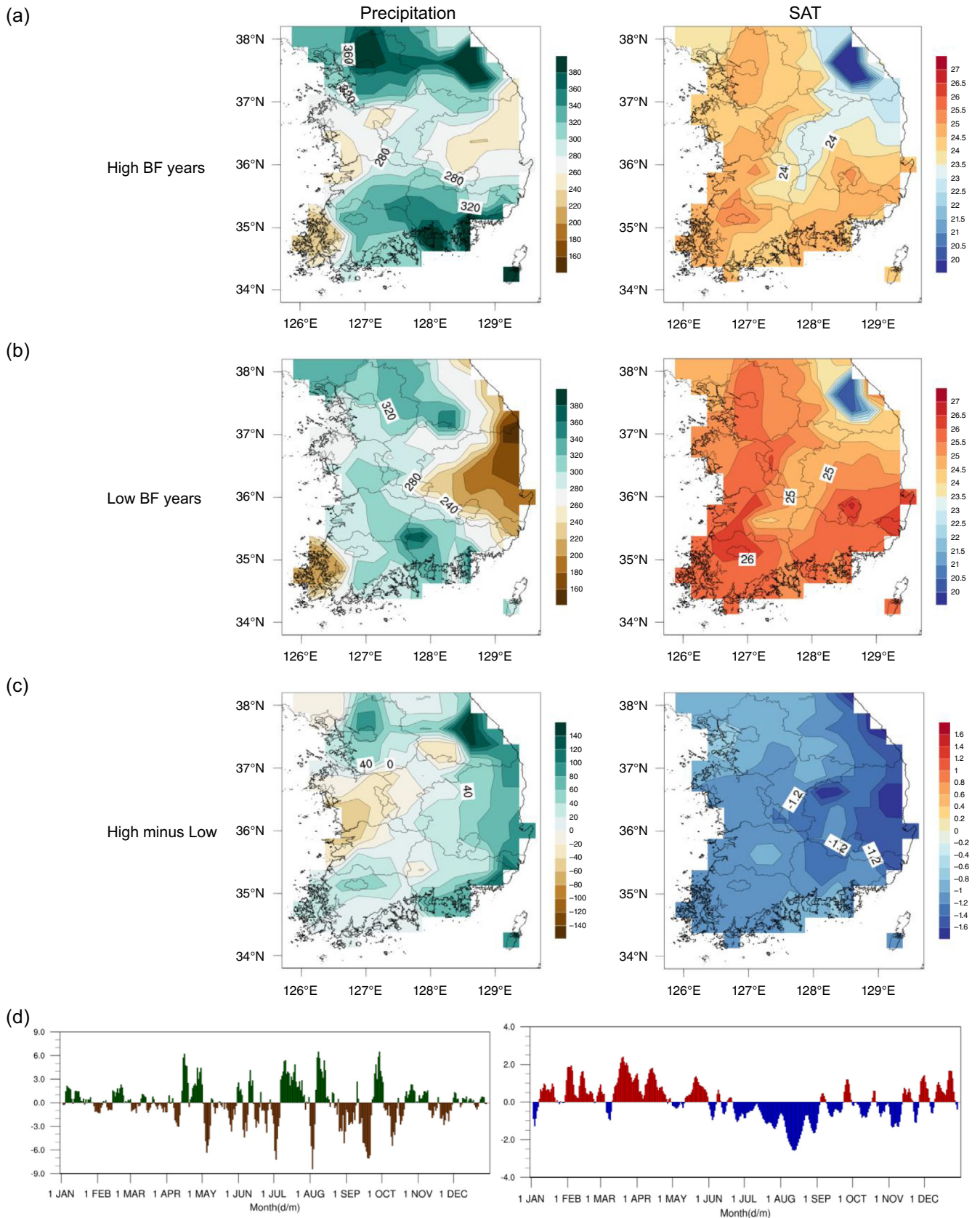


FIGURE 3 Spatial distributions of precipitation (mm) (left panel) and surface air temperature (SAT; °C) (right panel) in (a) high BF years, (b) low BF years and (c) high minus low BF years in JJA. (d) Daily time series of precipitation (mm) (left panel) and SAT (°C) (right panel) in high minus low BF years [Colour figure can be viewed at wileyonlinelibrary.com]

regions in the Tibetan Plateau showed a cold anomaly at the 95% confidence level, whereas most other regions, except for these two regions, showed a warm anomaly. The warm anomaly was significant in North Siberia at the 95% confidence level. In addition, the cold anomaly was particularly evident in NEA at the 95% confidence level. This means that Air2m was lower in all regions in NEA, including South Korea, during the summer high BF years. Thus, the time-series of area-averaged Air2m in NEA and blocking frequency were analysed (Figure 4b). The analysis results showed a steady positive trend in NEA until now. This positive trend was significant at the 90% confidence level. The trend of the blocking frequency was 0.06 yr^{-1} and the trend of Air2m was $0.02^\circ \text{Cyr}^{-1}$. The out-of-phase relationship was clear between the two variables. Accordingly, the correlation between the two variables was analysed. A negative correlation of -0.48 was revealed that significant at the 99% confidence level. As the blocking frequency increased in the OK region during summer, Air2m decreased in NEA. Even after removing the linear trends from the two time series, there was no significant difference from the original correlation coefficient ($r = -0.46$, which was significant at the 99% confidence level).

The present study compared the differences in summer air temperatures in the lower, middle and upper

troposphere in the two groups (left panel of Figure 5). A clear cold anomaly was revealed in NEA at the 850 hPa level at the 95% confidence level (left panel of Figure 5a). In particular, the largest warm anomaly was revealed in Northern Siberia at the 95% confidence level. At the 500 hPa level, the cold anomaly area was shifted slightly to the north (left panel in Figure 5b). On the other hand, the largest cold and warm anomalies were located in the NEA and North Siberia regions, respectively. At the 300 hPa level, the cold anomaly region was shifted much more to the north than that in the lower and middle troposphere (left panel of Figure 5c). Thus, NEA exhibited a weak warm anomaly, whereas the North Siberia region showed a strong cold anomaly.

This study compared the differences in the relative humidity in summer in the lower, middle and upper troposphere between the two groups (right panel of Figure 5). The analysis results showed a positive anomaly in Korea and Japan in the lower, middle and upper tropospheres. This was attributed to the effects of more precipitation in the high BF years than in the low BF years, as discussed above. This suggests that the high BF years were affected by colder and wetter air in NEA than in the low BF years.

This study also analysed the difference in the stream flows in summer in the lower, middle and upper

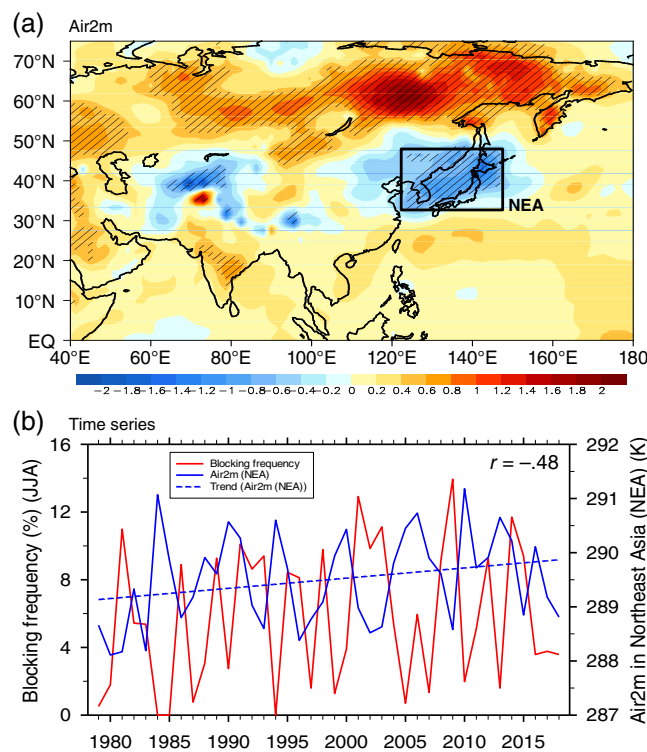


FIGURE 4 (a) Composite difference in 2 m air temperature (Air2m) between high BF years and low BF years in JJA and (b) time series of JJA BF and Air2m averaged over Northeast Asia (NEA; $32.5^\circ\text{--}47.5^\circ\text{N}$, $125.0^\circ\text{--}145.0^\circ\text{E}$). In (a), the hatched lines are significant at the 95% confidence level, and the unit is K [Colour figure can be viewed at wileyonlinelibrary.com]

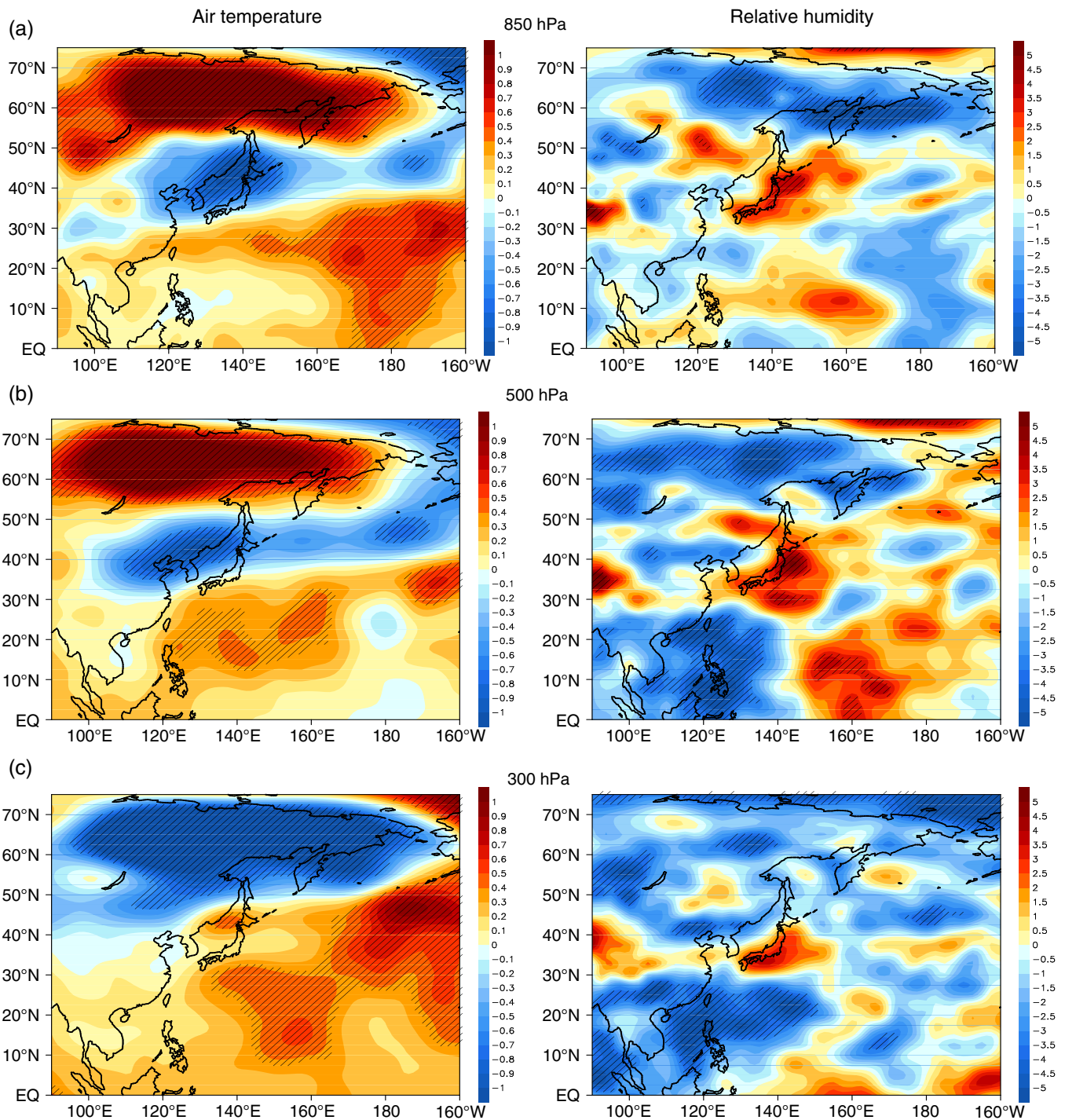


FIGURE 5 Composite differences in air temperature (left panel) and relative humidity (right panel) at (a) 850 hPa, (b) 500 hPa and (c) 300 hPa between high BF years and low BF years in JJA. The hatched lines are significant at the 95% confidence level. Units are $^{\circ}\text{C}$ for air temperature and % for relative humidity [Colour figure can be viewed at wileyonlinelibrary.com]

troposphere between the two groups (left panel of Figure 6). In all layers of the troposphere, strong anomalous anticyclonic circulations developed in the North Siberia region at the 95% confidence level, and anomalous cyclonic circulations developed in the NEA at the 95% confidence level. The anomalous anticyclone in the North Siberia region was related to the blocking high, while the anomalous cyclone

that developed in NEA was related to the East Asian summer monsoon (EASM) front. This was related to the decrease in the number of HWD because of the strong development of EASM precipitation in Korea when the blocking frequency increased in the OK region during summer. On the other hand, an anomalous southeasterly wind, which was characterized by warm air, was positioned in the

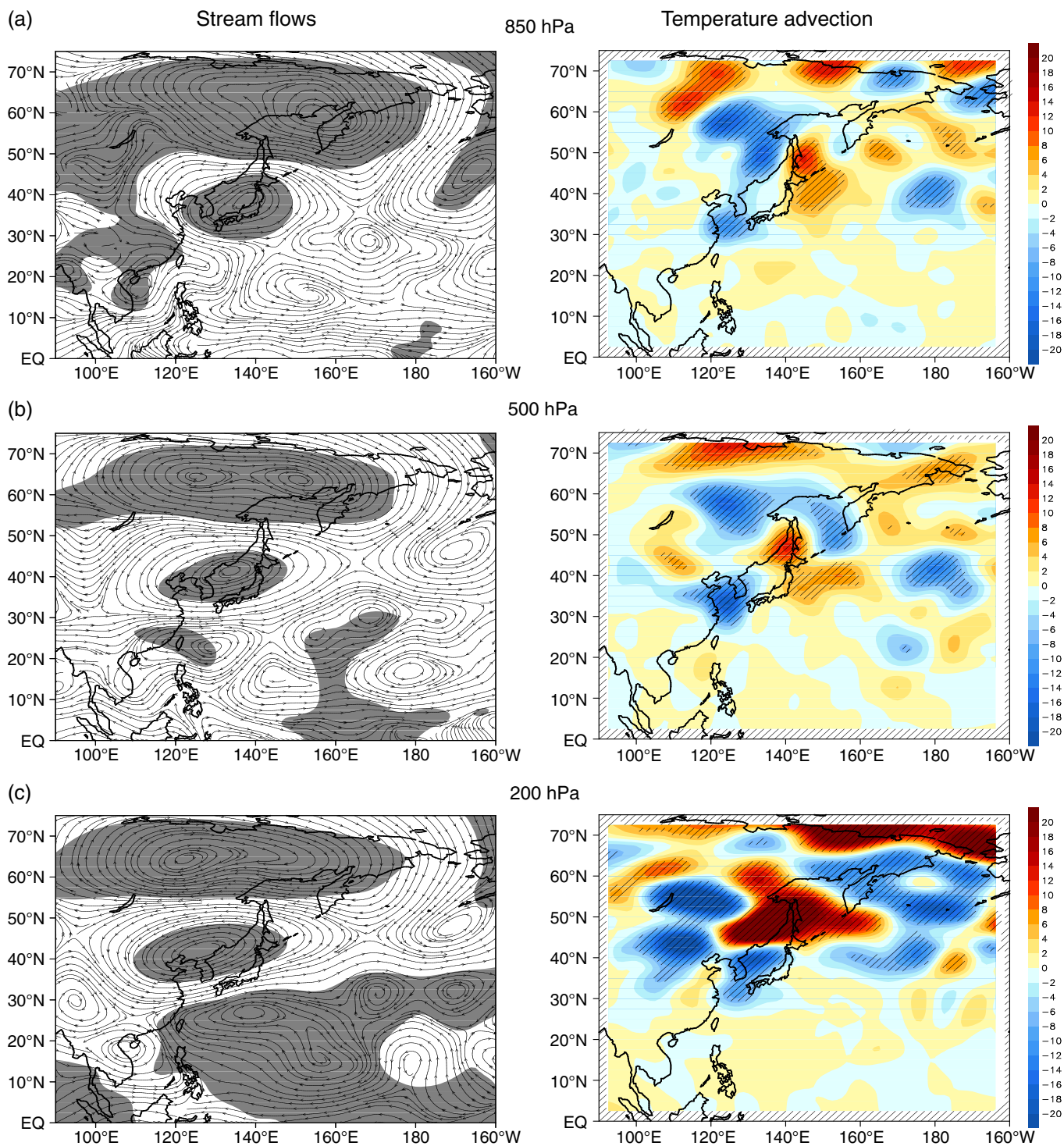


FIGURE 6 Composite differences in stream flows (left panel) and temperature advection (right panel) at (a) 850 hPa, (b) 500 hPa and (c) 200 hPa between high BF years and low BF years in JJA. The shaded areas in stream flows and hatched lines in temperature advection are significant at the 95% confidence level. The units of temperature advection are $^{\circ}\text{Cs}^{-1}$ [Colour figure can be viewed at wileyonlinelibrary.com]

North Siberia region. An anomalous southwesterly wind, which represented warm air, developed in NEA at the 850 hPa level, whereas an anomalous easterly wind or anomalous northeasterly wind, which represented cold air, developed in the North Siberia region.

This study analysed the difference in summer temperature advection in the lower, middle and upper troposphere between the two groups (right panel of Figure 6). The cold temperature advection anomaly was revealed in South Korea and the north and west sides of South Korea

in all layers of the troposphere at the 95% confidence level. This was attributed to the anomalous northwesterly wind, which was a cold air from the north and west sides of South Korea. This result was also related to the reduction in the number of HWDs in Korea when the blocking frequency increased in the OK region in summer.

The difference in the summer OLR between the two groups showed that the convection developed in the mid-latitude region of East Asia (Figure 7a). This was related to the EASM front. The convection was weakened in the west region of the western North Pacific (WNP), whereas the convection was strengthened in the east region of the WNP. The positive total cloud cover (TCDC) was present in NEA due to convection strengthening with regard to the difference in TCDC in summer between the two groups (Figure 7b). The positive anomaly was also present in the mid-latitude region in East Asia with regard

to the difference in the 850 hPa specific humidity between the two groups at the 95% confidence level (Figure 7c). As a result, positive precipitation was revealed in the mid-latitude region in East Asia with regard to the difference in summer precipitation between the two groups (Figure 7d). These results indicated that the increase in precipitation due to the convective strengthening in Korea during the high BF years led to a decrease in the number of HWDs. In addition, negative and positive precipitation anomalies were formed in the west and east regions of the WNP, respectively. The difference in the summer rain duration and Changma duration in Korea between the two groups was analysed (Table 2). The high BF years average rain duration was 42.6 days, and the average rain duration in the low BF years was 35.5 days, showing an approximately 7 days difference between the two groups. The average Changma duration in the high and low BF years was 36.0

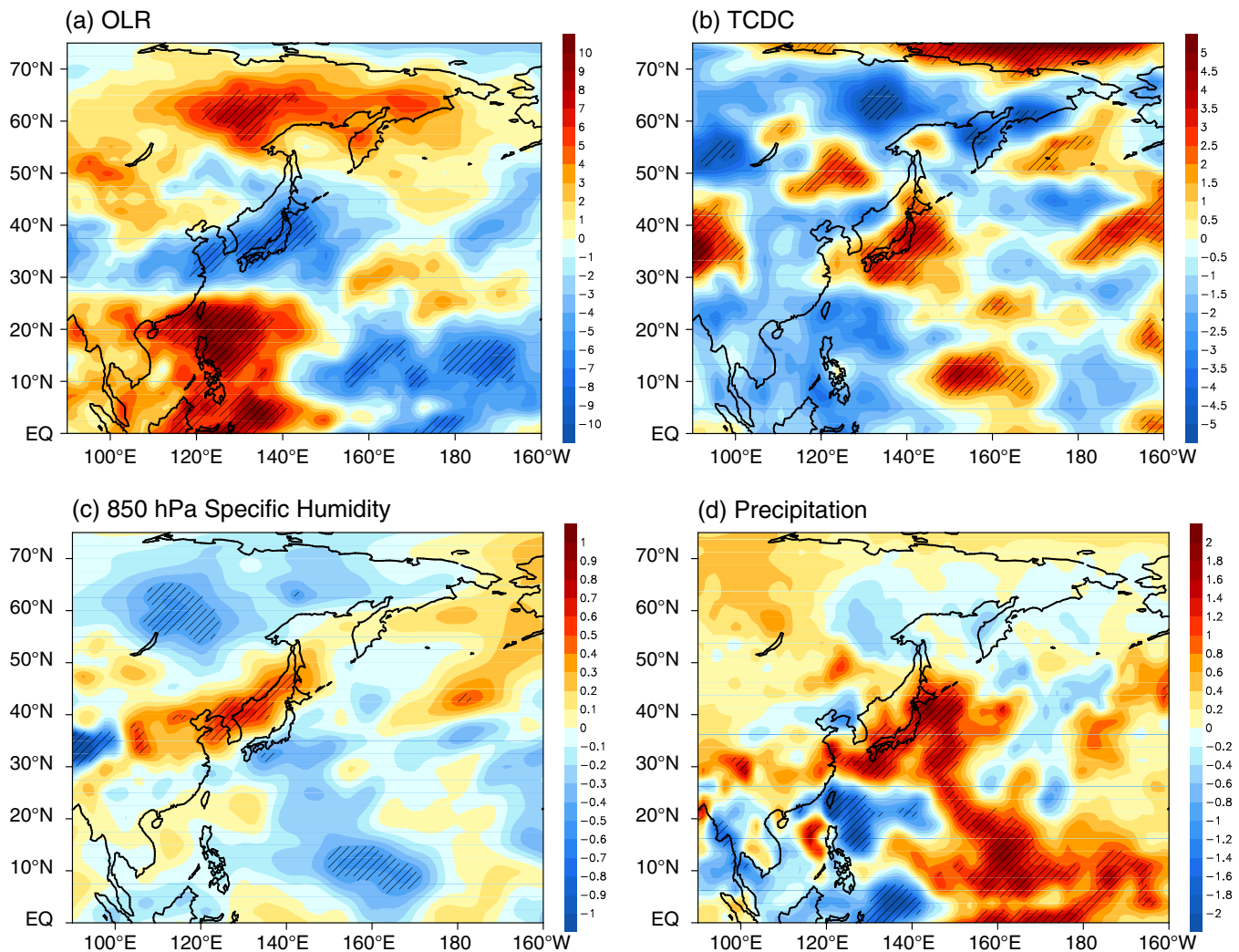


FIGURE 7 Composite differences in (a) OLR, (b) total cloud cover (TCDC), (c) 850 hPa specific humidity and (d) precipitation between high BF years and low BF years in JJA. The units are $\text{W}\cdot\text{s}^{-1}$ for OLR, % for TCDC, $\text{g}\cdot\text{kg}^{-1}$ for specific humidity and $\text{mm}\cdot\text{day}^{-1}$ for precipitation [Colour figure can be viewed at wileyonlinelibrary.com]

TABLE 2 Statistics of rain day and Changma duration on high and low BF years

High BF years			Low BF years		
Year	Rain day (JJA)	Changma duration	Year	Rain day (JJA)	Changma duration
1981	42.0	28	1979	40.0	30
1991	41.0	41	1984	36.7	25
1993	45.2	41	1985	34.9	23
1998	49.8	37	1987	41.9	37
2001	35.6	43	1994	23.8	21
2002	39.7	34	1997	22.5	29
2003	48.5	35	1999	37.5	20
2009	42.2	33	2005	39.0	19
2014	45.9	30	2007	41.6	35
2015	35.9	38	2013	37.1	44
Average	42.6	36.0	Average	35.5	28.3

and 28.3 days, respectively, showing that the average Change duration in the high BF years was 7 days longer than that of the low BF years. The difference in Changma duration between the two groups was significant at the 95% confidence level. Thus, the high BF years had longer rain and Changma durations, indicating that the longer durations may cause a greater reduction in the number of HWDs during the high BF years.

The difference in the vertical meridional circulation averaged over the NEA longitude (125°–145°E) between the two groups showed that anomalous upward flows developed in the latitudinal band of 30°–40°N, which is the latitude band where Korea is located (Figure 8a). In particular, the center of the anomalous upward flows strongly developed in 30°–35°N, where South Korea is located, in which the vertical velocity was significant at the 95% confidence level. This is consistent with the result showing that the precipitation in Korea increased in the high BF years as analysed above. The difference in the temperature averaged over the longitude (125°–145°E) of NEA displayed a cold anomaly at 30°–40°N, where Korea is located (Figure 8b). This was attributed to the increase in precipitation in Korea in the high BF years, as analysed above. This cold anomaly tended to tilt toward the north as it was closer to the upper troposphere. The difference in relative humidity averaged over the longitude (125°–145°E) of NEA between two groups showed a positive anomaly at 30°–50°N, and the strongest positive anomaly was located at 30°–40°N at the 95% confidence level, where Korea is positioned. This positive anomaly was attributed to the increase in precipitation in Korea in the high BF years, as analysed above.

This study also analysed the time series of the blocking frequency with a 500 hPa geopotential height (Z500),

TCDC, sensible heat net flux (SHTFL) and PDSI, which were area-averaged over Korea (32.5°–47.5°N, 125°–135°E; Figure 9a). First, Z500 tended to increase up until now, and the increasing tendency was significant at the 90% confidence level (uppermost panel of Figure 9a). The out-of-phase relationship with the blocking frequency was clear. Therefore, the correlation between the two variables was analysed. As a result, a negative correlation of -0.48 was revealed, which was significant at the 99% confidence level. This result suggests that when the blocking frequency increased in the OK region in summer, Z500 decreased in Korea. Second, TCDC tended to decrease up until now, which was significant at the 90% confidence level (second panel of Figure 9a). The in-phase relationship with the blocking frequency was clear. Thus, the correlation between the two variables was analysed. A positive correlation of 0.49 was observed, which was significant at the 99% confidence level. This means that as the block frequency increased in the OK region during summer, TCDC also increased in Korea. Third, SHTFL showed no significant trend change (third panel of Figure 9a). The out-of-phase relationship with the blocking frequency was clear. Thus, the correlation between the two variables was analysed. As a result, a negative correlation of -0.51 was revealed, which was significant at the 99% confidence level. This means that SHTFL decreased in Korea as the block frequency increased in the OK region during summer. Fourth, PDSI showed no significant trend change (fourth panel of Figure 9a). The in-phase relationship with the blocking frequency was clear. Thus, the correlation between the two variables was analysed. As a result, a positive correlation of 0.53 was revealed, which was significant at the 99% confidence level. Hence, drought in Korea was weakened as the block frequency increased in the OK

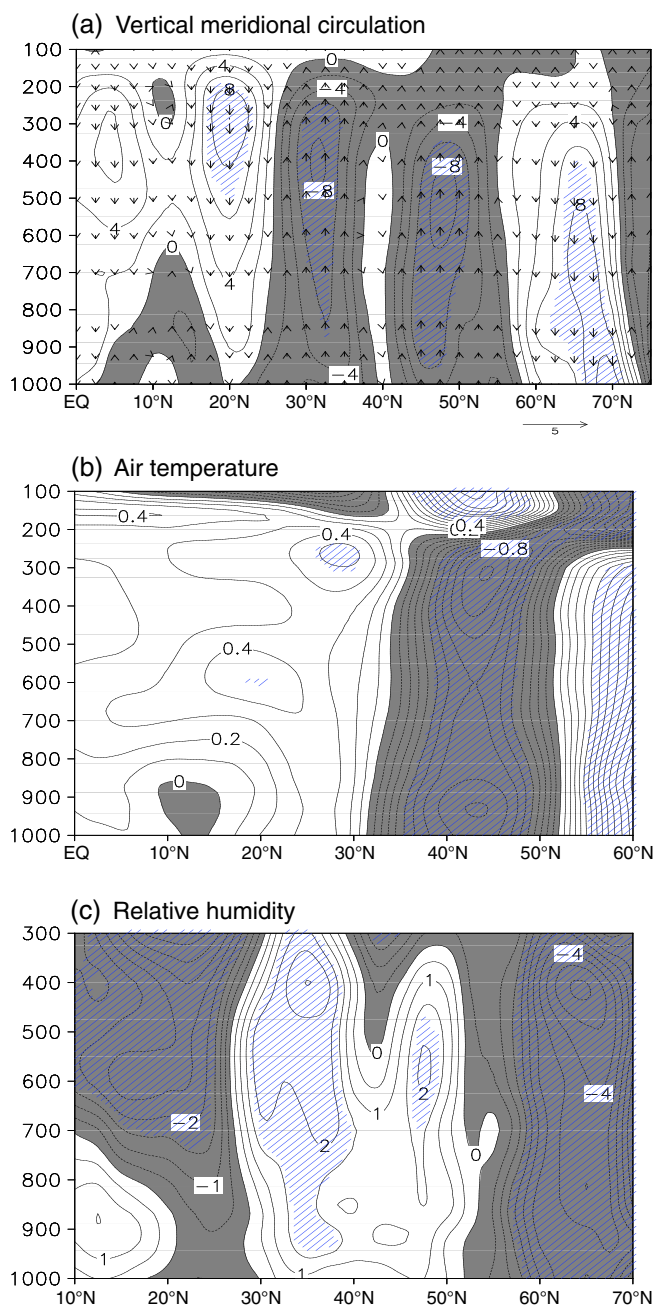


FIGURE 8 Composite differences of latitude–pressure cross-section of (a) vertical velocity (contours) and meridional circulations (vectors), (b) air temperature and (c) relative humidity averaged along 125° – 145° E between high and low BF years in JJA. The vertical velocity is multiplied by -100 . The dashed areas are significant at the 95% confidence level, and the shaded areas denote the negative values. Contour intervals are 2^{-2} hPa s^{-1} , 0.1°C , and 0.5% for the vertical velocity, air temperature and relative humidity, respectively [Colour figure can be viewed at wileyonlinelibrary.com]

region during summer. This was attributed to the result from the analysis of Z500, TCDC and SHTFL in precipitation in Korea also increased as the blocking frequency increased in the OK region in summer.

A correlation of HWD in Korea with Z500, TCDC, SHTFL and PDSI, which were area-averaged in Korea, was analysed (Figure 9b). A positive correlation of 0.73 was observed between the number of HWD and Z500, and a negative correlation of -0.53 was revealed between the number of HWDs and TCDC. A positive correlation of 0.48 was found between the number of HWDs and SHTFL, and a negative correlation of -0.57 was revealed between HWD and PDSI. The correlations of HWD with the four variables were all significant at the 99% confidence level. These results indicated that when Z500 and SHTFL decreased and TCDC increased in Korea, drought in Korea was weakened, and the number of HWDs decreased due to the increase in precipitation.

The reasons for the increase in precipitation in NEA during the high BF years were studied. Several studies reported that the EASM positively correlated with the snow cover in the East Asia continent (e.g. Liu and Yanai, 2002; Wu and Qian, 2003; Xiao and Duan, 2016). These studies showed that if the snow cover in the Eurasian continent during winter and spring showed a negative anomaly, the Tibetan high and WNPSH developed in summer by heating in the Eurasian continent, thereby strengthening EASM precipitation. Thus, the present study compared the snow cover in the Eurasian continent from March to May between the two groups (Figure 10a). The analysis result showed a negative snow cover anomaly in most regions in the Eurasia continent except for some regions of North Siberia and Tibetan Plateau. As a result, the difference in the ground heat net flux between the two groups showed a positive anomaly in most regions in the Eurasian continent except for some regions in the North Siberia and Tibetan Plateau (Figure 10b). This means that heating was strengthened in most regions in the Eurasian continent because of the low snow cover during spring. Accordingly, the WNPSH developed in the west up to the east coast of China and in the north up to the south coast of Japan. Moreover, the Tibetan high developed in the east up to 150°E and in the north up to the south coast of Korea during the high BF years (Figure 10c). The spatial distribution of WNPSH contributed to the formation of the EASM front in NEA and the precipitation by supplying a warm and wet southerly wind to the EASM front. Wei *et al.* (2014) revealed the influence of the eastward extension of the Tibetan High (the South Asian High) on the EASM rainfall. Furthermore, the eastward shift of the Tibetan High can lead to a westward extension of the WNPSH (Wei *et al.*, 2019). Therefore, the zonal shifts of these two high-pressure systems are not independent but related to each other. The precipitation that was strengthened in NEA during the high BF years was related to the reduction in the number of HWDs. On the other hand, WNPSH was

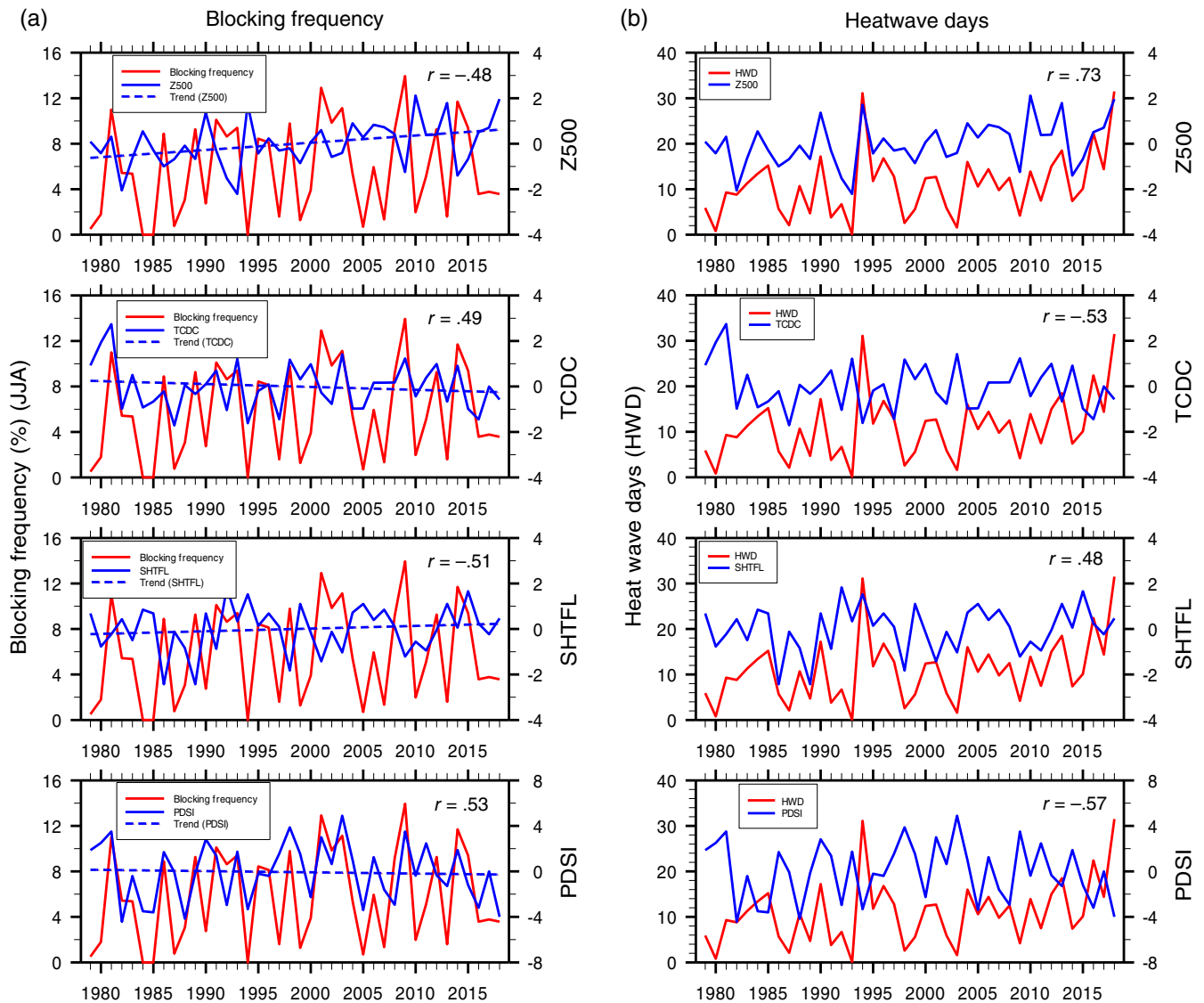


FIGURE 9 Time series of (a) JJA BF and Z500, TCDC, sensible heat net flux (SHTFL) and PDSI and (b) HWD in Korea (32.5° – 47.5° N, 125° – 135° E) and Z500, TCDC, SHTFL and PDSI [Colour figure can be viewed at wileyonlinelibrary.com]

weakened on the southeast side, and the Tibetan high was weakened on the southwest side during the low BF years (Figure 10d). The spatial distribution of these two high-pressure systems reduced the precipitation in NEA and heated the ground surface, helping to increase the number of HWDs.

The time-series of two variables with the EASM index were analysed to determine if the blocking frequency and the number of HWDs were related to the EASM (Figure 11). The EASM index tended to decrease slightly up until now, but the decrease was not statistically significant (Figure 11a). The in-phase relationship between the two variables was clear. Thus, the correlation between the two variables was analysed. A positive correlation of .51 was found, which was statistically significant at the 99% confidence level. Hence, the EASM was

strengthened as the block frequency increased in the OK region during summer. The out-of-phase relationship was clear between the number of HWDs and the EASM index. Thus, the correlation between the two variables was analysed (Figure 11b). As a result, a negative correlation of $-.53$ was revealed, which was significant at a 99% confidence level. This means that precipitation in Korea increased when the EASM was strengthened, thereby reducing the HWDs.

4.3 | North Atlantic oscillation

The difference in the SST between the two groups was analysed (Figure 12a). Overall, a warm anomaly was observed in most seas in the Indian Ocean and the Pacific

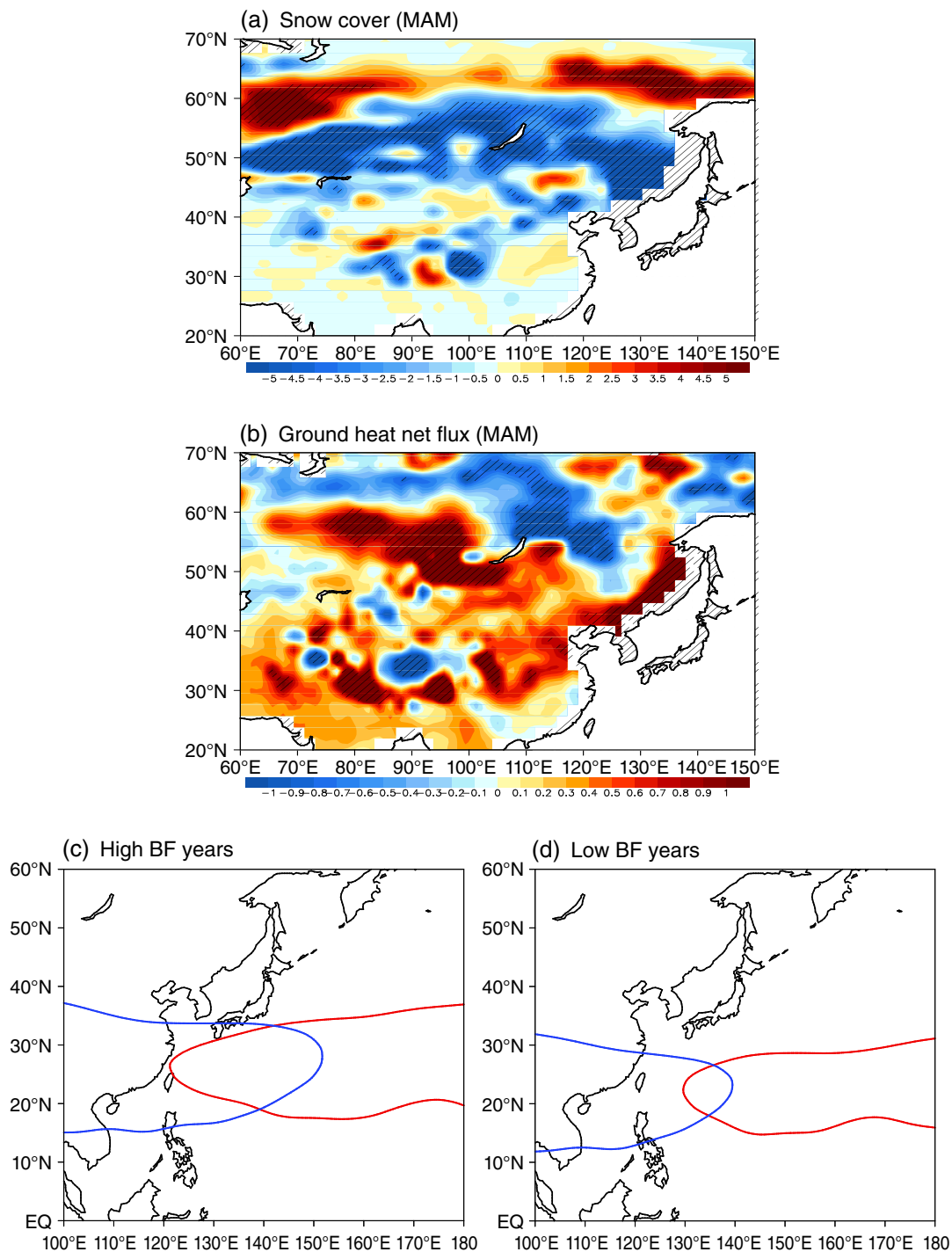


FIGURE 10 Composite difference in (a) snow cover (%) and (b) ground heat net flux ($\text{W}\cdot\text{m}^{-2}$) in March–May between high and low BF years. Spatial distribution of Tibetan high (blue line) and western North Pacific subtropical high (WNPSH; red line) in (c) high BF years and (d) low BF years in summer. Here, the Tibetan (WNPSH) high defines areas greater than 12,480 (5,875) gpm [Colour figure can be viewed at wileyonlinelibrary.com]

Ocean. A cold anomaly was noted in the seas near Korea and Japan due to the increased cloud and precipitation caused by the strengthening convection. Figure 12a also shows the eastern Pacific (EP) El Niño. On the other hand, a clear feature in Figure 12a is the El Niño. An El Niño in summer also makes the WNPSH

stretch westward, as shown in Figure 10c (Zhang *et al.*, 1999). In the North Atlantic Ocean, the tripole structure was revealed, where a cold anomaly in the high latitude, a warm anomaly in the mid-latitude, and a cold anomaly again in the low latitude were observed. This was a typical spatial distribution of the SST anomaly

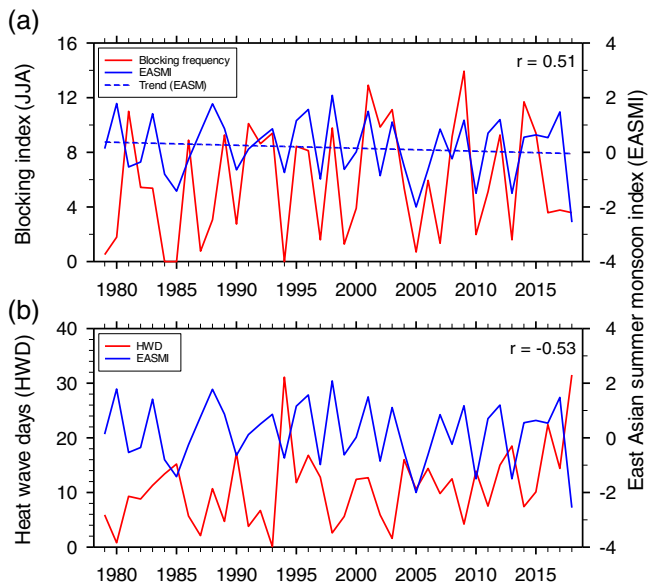


FIGURE 11 Time series of JJA east Asian summer monsoon index (EASMI) and (a) JJA BF and (b) HWD in Korea [Colour figure can be viewed at wileyonlinelibrary.com]

revealed in the positive North Atlantic Oscillation (NAO) phase. The analysis results of the difference in 500Z between the two groups also revealed an anomalous anticyclone in the mid-latitude region in the North Atlantic Ocean, and an anomalous cyclone in the high latitude region (Figure 12b). The Rossby wave train from these two pressure systems was propagated to the east. The anomalous atmospheric circulation was a typical pattern shown in the positive NAO phase. This study defined the North Atlantic index (NAI) as the difference in SST in area A, which was the warm anomaly region in the mid-latitudes of the North Atlantic Ocean, and area B, which was the cold anomaly region in the high latitude region. The time series of the NAI with the blocking frequency and HWDs in Korea were analysed. The NAI had no significant trend change up until now (Figure 12c). A clear in-phase relationship was observed between the NAI and blocking frequency. Thus, the correlation between the two variables was analysed. As a result, a positive correlation of .46 was revealed, which was significant at the 99% confidence level. This means that the blocking frequency in the OK region in summer increased as the SST increased in the mid-latitudes of the North Atlantic Ocean. The out-of-phase relationship between the NAI and HWDs in Korea was clear. Thus, the correlation between the two variables was analysed (Figure 12d). As a result, a negative correlation of -0.52 was noted, which was significant at the 99% confidence level. This means that the number of HWDs in Korea decreased as the SST increased in the mid-latitudes of the North Atlantic Ocean.

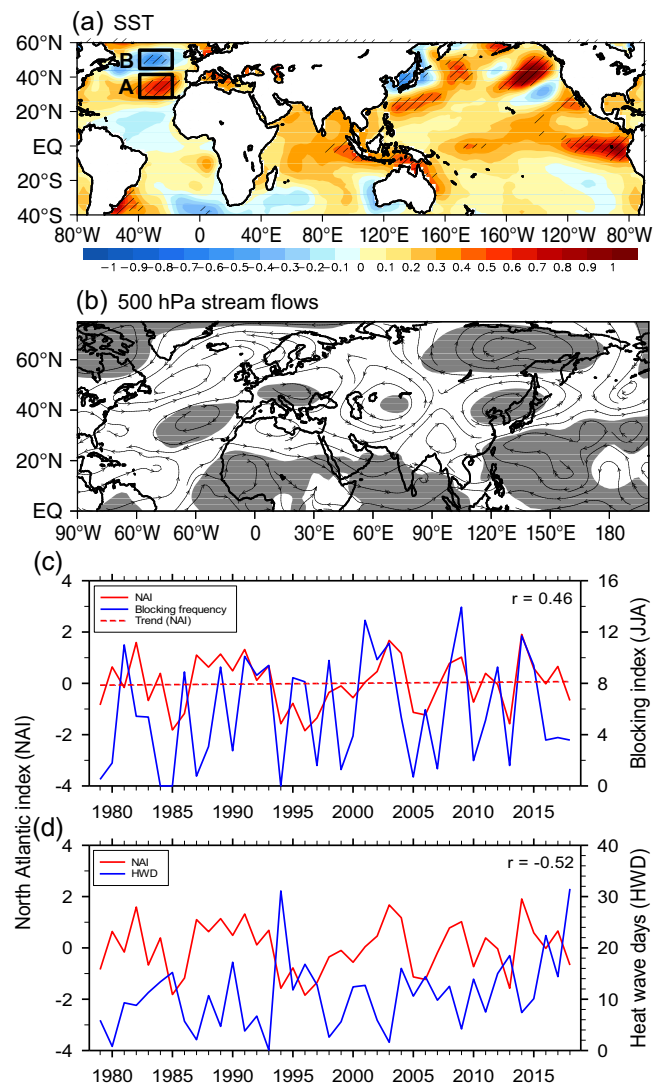


FIGURE 12 Composite differences in (a) SST and (b) 500 hPa stream flows. Time series of North Atlantic index (NAI; area A (27.5° – 40° N, 40° – 30° W) minus B (42.5° – 57.5° N, 40° – 30° W) and (c) JJA BF and (d) HWD in Korea. The hatched areas in (a) and shaded areas in (b) are significant at the 95% confidence level [Colour figure can be viewed at wileyonlinelibrary.com]

5 | SUMMARY AND CONCLUSION

This study examined the relationship between heatwaves in Korea and blocking during June to August in the OK region, which has had the most significant influence on the Korean climate in summer in the last 40 years (1979–2018). The correlations between the blocking frequency in the OK region during summer and the number of HWDs, TND and SAT in Korea during June to August were analysed, and negative correlations were found between them. These negative correlations suggest that when the blocking frequency increased in summer, the number of HWDs, TND and SAT in Korea decreased.

To explain the reduction in the number of HWD in Korea when the blocking frequency in the OK region increased in summer, this study selected 10 high blocking frequency years (high BF years) and 10 low blocking frequency years (low BF years), and the difference between the two groups were analysed. According to the difference in the Air2m in Asia during summer between the high and low BF years, NEA and some regions in the Tibetan Plateau showed cold anomalies, whereas most other regions showed warm anomalies. The warm anomaly was evident in North Siberia. In addition, the cold anomaly was particularly evident in NEA. This suggests that Air2m was lower in all regions in NEA, including South Korea, during the summer high BF years. Thus, the correlation between area-averaged Air2m in NEA and blocking frequency was analysed. A negative correlation of -0.48 was found, which means that in NEA, Air2m decreased with increasing blocking frequency in the OK region during summer.

According to the difference in summer air temperatures in the lower, middle and upper troposphere between the high and low BF years, a cold anomaly was observed in NEA at the 850 hPa level, whereas a warm anomaly appeared in the remaining regions. In particular, the largest warm anomaly was revealed in North Siberia. The cold anomaly was shifted slightly to the north at the 500 hPa level. On the other hand, the largest cold and warm anomalies were located in NEA and North Siberia regions, respectively. At the 300 hPa level, the cold anomaly region was shifted much more to the north than that in the lower and middle troposphere.

The difference in the summer relative humidity in the lower, middle and upper troposphere between the two groups showed a positive anomaly in Korea and Japan. This was attributed to the effects of enhanced precipitation in the high BF years compared to the low BF years.

According to the difference in summer stream flows in the lower middle and upper troposphere between the two groups, in all layers of the troposphere, anomalous anticyclonic circulations developed in the North Siberia region, and strong anomalous cyclonic circulations developed in NEA. In particular, the anomalous large anticyclone was related to the blocking high in North Siberia, and the anomalous cyclone that developed in NEA was related to the EASM front. This was related to the decrease in HWDs in Korea because of the increase in precipitation with the strong development of EASM when the blocking frequency increased in the OK region during summer.

The present study also analysed the difference in summer temperature advection in the lower, middle and upper troposphere between the high and low BF years. The cold temperature advection anomaly appeared in

South Korea and the north and west sides of South Korea in all layers of the troposphere. The anomaly was attributed to the anomalous northwesterly wind, which was cold air from the north and west sides of South Korea. This result was also related to the decrease in HWDs in Korea when the blocking frequency increased in the OK region in summer.

The difference in the summer OLR between the high and low BF years showed that convection was developed in the mid-latitude region of East Asia. This was related to the EASM front. Hence, in the west and east region of the WNP, the convection was weakened and strengthened, respectively. As a result, enhanced precipitation was revealed in the mid-latitude region in East Asia in the high BF years. These results suggest that the increase in precipitation due to convective strengthening in Korea during the high BF years led to a decrease in the number of HWDs.

According to the difference in the vertical meridional circulation averaged over the NEA longitude (125° – 145° E) between the two groups, anomalous upward flows developed in the latitudinal band of 30° – 40° N, where Korea was located. In particular, the center of the anomalous upward flows was developed strongly at 30° – 35° N, where South Korea was located. The difference in the air temperature averaged over the longitude of NEA displayed a cold anomaly at 30° – 40° N, where Korea is located. This was attributed to the increase in precipitation in Korea in the high BF years, as shown above. The difference in the relative humidity averaged over the longitude of NEA between the two groups showed a positive anomaly at 30° – 50° N. The strongest positive anomaly was located at 30° – 40° N, which was attributed to the increase in precipitation in Korea in the high BF years.

The difference in snow cover in the Eurasian continent during spring between the high and low BF years was also analysed. The analysis results showed a negative snow cover anomaly in most regions in the Eurasia continent except for some regions of North Siberia and the Tibetan Plateau. As a result, the difference in the ground heat net flux between the two groups revealed a positive anomaly in most regions in the Eurasian continent except for some regions in North Siberia and the Tibetan Plateau. This suggests that heating was strengthened in most regions in the Eurasian continent because of the low snow cover during spring. Accordingly, the WNPSH developed in the west up to the east coast of China and in the north up to the south coast of Japan, and the Tibetan high developed in the east up to 150° E and in the north up to the south coast of Korea during the high BF years. During the low BF years, however, WNPSH weakened on the southeast side, and the Tibetan high weakened on the southwest side.

The correlation of the EASM index with two variables was analysed to determine if the EASM was correlated with the blocking frequency and HWD. The analysis result showed a positive correlation of .51 between the blocking frequency and the EASM index. Hence, the EASM was strengthened as the blocking frequency increased in the OK region during summer. A negative correlation of $-.53$ was revealed between HWD and EASM index, indicating that precipitation increased in Korea when the EASM was strengthened, thereby reducing the HWDs.

According to the difference in the SST between the two groups, in the North Atlantic Ocean, the tripole structure appeared with cold anomalies in the high and low latitudes and a warm anomaly in the mid-latitude. This was a typical spatial distribution of SST anomalies revealed in the positive NAO phase. The difference in 500Z between the two groups also showed that anomalous anticyclonic and cyclonic circulations were placed in the mid and high latitudes in the North Atlantic Ocean, respectively, which is a typical atmospheric circulation pattern of the positive NAO phase.

HWDs are becoming more frequent in Korea. Although they are connected to blocking, other factors play a role, such as EASM, snow cover on the East Asian continent, and NAO. In a warming climate, it is vital to know the impacts of HWDs by understanding the connection of HWDs and using them to predict summer blocking in the Sea of Okhotsk and snow cover on the East Asian continent.

ACKNOWLEDGEMENTS

This work was carried out with the support of ‘Cooperative Research Program for Agriculture Science & Technology Development (Project No. PJ01489102)’ Rural Development Administration, Republic of Korea

AUTHOR CONTRIBUTIONS

Jae-Won Choi: Writing – original draft. **Chan-Yeong Song:** Visualization. **Eung-Sup Kim:** Validation. **Joong-Bae Ahn:** Project administration; writing – review and editing.

ORCID

Chan-Yeong Song  <https://orcid.org/0000-0002-8444-3938>

Joong-Bae Ahn  <https://orcid.org/0000-0001-6958-2801>

REFERENCES

- Adler, R.F., Huffman, G.J., Chang, A., Ferraro, R., Xie, P., Janowiak, J., Rudolf, B., Schneider, U., Curtis, S., Bolvin, D., Gruber, A., Susskind, J., Arkin, P. and Nelkin, E. (2003) The Version-2 global precipitation climatology project (GPCP) monthly precipitation analysis (1979-present). *Journal of Hydrometeorology*, 4, 1147–1167.
- Barriopedro, D., García-Herrera, R., Lupo, A.R. and Hernández, E. (2006) A climatology of northern hemisphere blocking. *Journal of Climate*, 19, 1042–1063. <https://doi.org/10.1175/JCLI3678.1>.
- Byun, H.R., Hwang, H.S. and Ko, H.Y. (2006) Characteristics and synoptic causes on the abnormal heat occurred at Miryang in 2004. *Atmosphere*, 16, 187–201 (In Korean with English abstract).
- Choi, Y.W. and Ahn, J.B. (2017) The effect of boreal late autumn snow cover over Western and Central China on the northern hemisphere wintertime blocking frequency. *Journal of Climate*, 30, 9027–9039. <https://doi.org/10.1175/JCLI-D-16-0830.1>.
- Ha, K.J., Yeo, J.H., Seo, Y.W. and Chung, W.S. (2020) What caused the extraordinarily hot 2018 summer in Korea? *Journal of the Meteorological Society of Japan*, 98, 153–167.
- Hong, J.S., Yeh, S.W. and Seo, K.H. (2018) Diagnosing physical mechanisms leading to pure heat waves versus pure tropical nights over the Korean peninsula. *Journal of Geophysical Research*, 123, 7149–7160. <https://doi.org/10.1029/2018JD028360>.
- Kanamitsu, M., Ebisuzaki, W., Woollen, J., Yang, S.K., Hnilo, J.J., Fiorino, M. and Potter, G.L. (2002) NCEP-DOE AMIP-II reanalysis (R-2). *Bulletin of the American Meteorological Society*, 83, 1631–1643.
- Kim, Y.S. and Hong, S.G. (1996) A study of quasi-Föhn in the Youngdong-district in late spring or early summer. *Journal of the Korean Meteorological Society*, 32, 593–600 (In Korean with English abstract).
- Kim, S.Y. and Min, K.D. (2001) Effects of terrain and land-use on local circulation and temperature change at Taegu region in summer. *Journal of the Korean Meteorological Society*, 37, 487–512.
- Kim, H.G., Min, K.D., Yoon, I.H., Moon, Y.S. and Lee, D.I. (1998) Characteristics of the extraordinary high temperature events occurred in summer of 1987 and 1994 over the Korean peninsula. *Journal of the Korean Meteorological Society*, 34, 47–64 (In Korean with English abstract).
- Kim, M.K., Oh, J.S., Park, C.K., Min, S.K., Boo, K.O. and Kim, J.H. (2019) Possible impact of the diabatic heating over the Indian subcontinent on heat waves in South Korea. *International Journal of Climatology*, 39, 1166–1180.
- Lee, H.Y. (1994) Föhn phenomenon on the Yeong-Seo. *Journal of the Korean Geographical Society*, 29, 266–280.
- Lee, S. (2003) Difference of air temperature between the west and east coast regions of Korea. *Journal of the Korean Meteorological Society*, 39, 43–57.
- Lee, D.Y. and Ahn, J.B. (2017) Future change in the frequency and intensity of wintertime North Pacific blocking in CMIP5 models. *International Journal of Climatology*, 37, 2765–2781. <https://doi.org/10.1002/joc.4878>.
- Lee, W.S. and Lee, M.I. (2016) Interannual variability of heat waves in South Korea and their connection with large-scale atmospheric circulation patterns. *International Journal of Climatology*, 36, 4815–4830.
- Li, J.P. and Zeng, Q.C. (2002) A unified monsoon index. *Geophysical Research Letters*, 29, 1274. <https://doi.org/10.1029/2001GL013874>.
- Li, J.P. and Zeng, Q.C. (2003) A new monsoon index and the geographical distribution of the global monsoons. *Advances in Atmospheric Sciences*, 20, 299–302.

- Li, J.P. and Zeng, Q.C. (2005) A new monsoon index, its inter-annual variability and relation with monsoon precipitation. *Climatic and Environmental Research*, 10, 351–365.
- Liebmann, B. and Smith, C.A. (1996) Description of a complete (interpolated) outgoing longwave radiation dataset. *Bulletin of the American Meteorological Society*, 77, 1275–1277.
- Lim, W.I. and Seo, K.H. (2019) Physical-statistical model for summer extreme temperature events over South Korea. *Journal of Climate*, 32, 1725–1742.
- Liu, X. and Yanai, M. (2002) Influence of Eurasian spring snow cover on Asian summer rainfall. *International Journal of Climatology*, 22, 1075–1089.
- National Institute of Meteorological Studies (NIMS). (2016). 100 Years of Climate Change and Future Prospects on the Korean Peninsula
- Park, Y.J. and Ahn, J.B. (2014) Characteristics of atmospheric circulation over East Asia associated with summer blocking. *Journal of Geophysical Research – Atmospheres*, 119, 726–738. <https://doi.org/10.1002/2013JD020688>.
- Smith, T.M., Reynolds, R.W., Peterson, T.C. and Lawrimore, J. (2008) Improvements to NOAA's historical merged land-ocean surface temperature analysis (1880–2006). *Journal of Climate*, 21, 2283–2296.
- Tibaldi, S. and Molteni, F. (1990) On the operational predictability of blocking. *Tellus*, 42A, 343–365. <https://doi.org/10.1034/j.1600-0870.1990.t01-2-00003.x>.
- Wei, W., Zhang, R., Wen, M., Rong, X. and Li, T. (2014) Impact of Indian summer monsoon on the south Asian high and its influence on summer rainfall over China. *Climate Dynamics*, 43, 1257–1269.
- Wei, W., Zhang, R., Wen, M., Yang, S. and Li, W. (2019) Dynamic effect of south Asian high on the interannual zonal extension of the western North Pacific subtropical high. *International Journal of Climatology*, 39, 5367–5379.
- Wilks, D.S. (1995) *Statistical Methods in the Atmospheric Sciences*. New York, NY: Academic Press, p. 467.
- Wu, T.W. and Qian, Z.A. (2003) The relation between Tibetan winter snow and the Asian summer monsoon and rainfall: an observational investigation. *Journal of Climate*, 16, 2038–2051.
- Xiao, Z. and Duan, A. (2016) Impact of Tibetan plateau snow cover on the interannual variability of the east Asian summer monsoon. *Journal of Climate*, 29, 8495–8514.
- Yeh, S.W., Won, Y.J., Hong, J.S., Lee, K.J., Kwon, M.H., Seo, K.H. and Ham, Y.G. (2018) The record-breaking heat wave in 2016 over South Korea and its possible mechanism. *Monthly Weather Review*, 146, 1463–1474.
- Yeo, S.R., Yeh, S.W. and Lee, W.S. (2019) Two types of heat wave in Korea associated with atmospheric circulation pattern. *Journal of Geophysical Research*, 124, 7498–7511.
- Yoon, D., Cha, D.H., Lee, M.I., Min, K.H., Kim, J.W., Jun, S.Y. and Choi, Y. (2020) Recent changes in heatwave characteristics over Korea. *Climate Dynamics*, 55, 1685–1696.
- You, J.E. and Ahn, J.B. (2012) The anomalous structures of atmospheric and oceanic variables associated with the frequency of North Pacific winter blocking. *Journal of Geophysical Research – Atmospheres*, 117, D11108. <https://doi.org/10.1029/2012JD017431>.
- Zhang, R., Sumi, A. and Kimoto, M. (1999) A diagnostic study of the impact of El Niño on the precipitation in China. *Advances in Atmospheric Sciences*, 16, 229–241.

How to cite this article: Choi, J.-W., Song, C.-Y., Kim, E.-S., & Ahn, J.-B. (2022). Possible relationship between heatwaves in Korea and the summer blocking frequency in the Sea of Okhotsk. *International Journal of Climatology*, 1–19. <https://doi.org/10.1002/joc.7659>